Systems/Circuits

Neural Correlates of Online Action Preparation

Mahdiyar Shahbazi,[1] Giacomo Ariani,[1,2] Mehrdad Kashefi,[1] J. Andrew Pruszynski,[1,3] and Jörn Diedrichsen[1,2,4]
[1]Western Institute for Neuroscience, Western University, London, Ontario N6A 3K7, Canada and Departments of [2]Computer Science, [3]Physiology and Pharmacology, and [4]Statistical and Actuarial Sciences, Western University, London, Ontario N6A 3K7, Canada

When performing movements in rapid succession, the brain needs to coordinate ongoing execution with the preparation of an upcoming action. Here we identify the processes and brain areas involved in this ability of online preparation. Human participants (both male and female) performed pairs of single-finger presses or three-finger chords in rapid succession, while 7T fMRI was recorded. In the overlap condition, they could prepare the second movement during the first response and in the nonoverlap condition only after the first response was completed. Despite matched perceptual and movement requirements, fMRI revealed increased brain activity in the overlap condition in regions along the intraparietal sulcus and ventral visual stream. Multivariate analyses suggested that these areas are involved in stimulus identification and action selection. In contrast, the dorsal premotor cortex, known to be involved in planning upcoming movements, showed no discernible signs of heightened activity. This observation suggests that the bottleneck during simultaneous action execution and preparation arises at the level of stimulus identification and action selection, whereas movement planning in the premotor cortex can unfold concurrently with the execution of a current action without requiring additional neural activity.

Key words: **action selection; fMRI; hand control; motor planning; MVPA; sequential movements**

Significance Statement

The brain's ability to select and plan upcoming actions while controlling ongoing movements is a crucial evolutionary adaptation of the action system. However, the neural basis of online action preparation remains largely unknown. We found that superior parietal and occipitotemporal areas exhibited heightened activation during online preparation. Surprisingly, the dorsal premotor cortex, known to be a crucial structure in motor planning, did not display additional activation during online preparation. These findings imply that while motor planning within the premotor cortex can occur in parallel with the execution of an ongoing movement, stimulus identification and action selection in the posterior parietal cortex constitute a bottleneck for online action preparation.

Introduction

Most laboratory studies of perception, action, or decision-making consist of distinct trials: a sequence of stimulus, response, and feedback is followed by a short pause before the next trial begins. In contrast, most tasks in real life involve a continuous stream of actions. For example, imagine you are trying to play a piece of music on a piano from a sheet of music, aiming to press the right keys with the correct timing. The process of preparing the next chord (Fig. 1*A*) consists of the identification of the stimulus, the selection of the correct chord (Rosenbaum and Kornblum, 1982), and the planning of the correct motor action (Shenoy et al., 2013). One possible strategy would be to prepare only one chord at a time, execute it, and then prepare the next chord. However, this strategy fails if there is not enough time to prepare the next chord after playing the current one. In such situations, one needs to start preparing future movements before the current movement is completed. A series of recent studies show that participants indeed engage in this process of online preparation (Ariani et al., 2021; Kashefi et al., 2023), selecting and planning 2–3 movements ahead of the current action. However, how the brain coordinates the preparation of future movements with the simultaneous execution of ongoing movement remains unknown.

Electrophysiological recordings in primary motor and premotor regions have shown that the same areas and often even the same neurons are engaged in both preparation and subsequent execution of a single movement (Tanji and Evarts, 1976; Crammond and Kalaska, 1994, 2000; Churchland and Shenoy, 2007; Ames et al., 2014; Pruszynski et al., 2014). Given this overlap, how does the brain coordinate the execution of one movement with the simultaneous preparation of another? One

Received Oct. 4, 2023; revised April 9, 2024; accepted April 12, 2024.
Author contributions: M.S., G.A., M.K., J.A.P., and J.D. designed research; M.S. performed research; M.S. contributed unpublished reagents/analytic tools; M.S. analyzed data; M.S. and J.D. wrote the paper.
This work was supported by a Canadian Institutes of Health Research Project Grant to J.D. and J.A.P. (PJT-175010) and the Canada First Research Excellence Fund (BrainsCAN).
The authors declare no competing financial interests.
Correspondence should be addressed to Jörn Diedrichsen at jdiedric@uwo.ca.
https://doi.org/10.1523/JNEUROSCI.1880-23.2024

possibility is that these two processes rely on independent sets of neurons or independent dimensions of the neuronal state space (Kaufman et al., 2014), enabling those processes to run in parallel without interference (Zimnik and Churchland, 2021). Alternatively, the two processes might interfere with each other, and the brain may resolve this conflict by recruiting additional neuronal resources, either through the activation of more neurons within the same regions or by involving previously unengaged areas.

Here we test whether the human visuomotor system shows extra BOLD activity during online preparation. We designed a high-field (7 T) fMRI experiment in which participants performed a series of finger presses in response to arbitrary visual cues. In the "overlap" condition, the next movement was cued during the current action. In the "nonoverlap" condition, the same actions occurred sequentially. The behavioral results showed that participants used the overlap for online preparation. Because overlap and nonoverlap conditions were matched for basic perceptual and execution requirements, differences in activity can be attributed to extra processes engaged during online preparation.

We also wanted to determine at which stage of online preparation the extra activity may occur. Traditionally, action preparation has been subdivided into the process of stimulus identification, action selection, and motor planning (Rosenbaum and Kornblum, 1982). However, recent research has shown that the boundaries between these processes are more fluid, with motor planning being able to start before action selection is completed (Cisek and Kalaska, 2010). We therefore did not attempt to subdivide preparation into discrete stages but rather consider action preparation to be a continuous process that changes from stimulus- to action-related. To identify where along this continuum the extra activity occurred, we varied the motoric complexity of the movements from single-finger presses to a chord of three-finger presses. Experiment 1 confirmed that action preparation for chords requires more time than for single-finger presses. In Experiment 2, we then compared the activity related to online preparation between the chord and single-finger conditions. Additionally, we counterbalanced the stimulus-to-response mapping across participants and used multivariate techniques to determine whether the regions that showed extra activity during online planning were related to cue or action processing.

Materials and Methods

Participants. A total of 11 individuals (four females; mean age, 26 ± 4) participated in Experiment 1, and 22 individuals (12 females; mean age, 24 ± 4) participated in Experiment 2. Four individuals participated in both experiments. Inclusion criteria required right-handedness and no history of psychiatric or neurological disorders. Participants provided written informed consent to all procedures and data usage before the study started, and all the experimental procedures were approved by the Human Research Ethics Board at Western University.

Apparatus. Finger presses were produced on a right-hand MRI–compatible keyboard with five 10.5 × 2 cm keys. Each key had an indentation to guide fingertip placement. Finger presses were isometric. Forces were measured by transducers (FSG-15N1A; Sensing and Control Honeywell; the dynamic range of 0–25 N; update rate, 5 ms) located beneath the fingertip indentation of each key. To register a key press, the applied force had to exceed the 0.8 N threshold, indicated by a horizontal red line on the top of the screen (Fig. 1*B*). Five white lines were displayed on a computer screen such that the vertical position of each line was proportional to the force exerted by each finger on the respective key (Fig. 1*C*). In Experiment 2, the visual stimuli (symbols) were presented in the two vertically aligned boxes with a fixation cross between them (Fig. 2*A*). The distance between the symbols and fixation was ∼1°.

Paced response task (general procedures). In both experiments, the task required participants to produce responses at a fixed pace. The responses were either single-finger or simultaneous three-finger presses (chord). For each of these, we assigned five arbitrary symbols to the five responses (Fig. 1*B*). The five chords consisted of different combinations of pressing three of five fingers. The chords (135, 145, 235, 245, and 345) were used with 1 indicating the thumb and 5 the pinkie finger. After learning the symbol-to-action mapping, participants were trained to produce the three-finger presses simultaneously, so the chord could be produced as a single unit. During scanning, the average absolute asynchrony between the time when each finger crossed the force threshold was 16 ms (±2 ms, ± indicating the SEM across participants).

To help participants keep a regular pace, we presented a sequence of high- and low-pitch tones. Similar to the "forced-response" paradigm (Haith et al., 2016), participants had to respond synchronously with the high-pitch tones. The response time was defined as the time point when the summed force across fingers reached its peak.

To provide feedback on the temporal accuracy of the response, we displayed a bar in the lower part of the screen (Fig. 1*C*). If the response was too early, the bar pointed to the left, and if the response was too late, the bar pointed to the right. The length of the bar indicated the size of the deviation. The acceptable deviation (200 ms) was specified by the box boundaries. If the executed response matched the instructed cue, the bar appeared in green; otherwise, it appeared in red, indicating an error.

Points were awarded for each press and time accuracy according to the following scheme: −2 points in case of timing error (deviation >200 ms); 0 points for pressing any wrong key without timing error; and 1 point in case of a correct response without timing error.

Experiment 1. The purpose of this experiment was to quantify the time necessary to prepare a single finger or chord movement, respectively. At the beginning of the experiment, participants were trained in symbol-to-action mapping. In separate runs for single-finger and chord, we presented a symbol on the screen and asked them to produce the corresponding response. We encouraged them to delay their response until they felt confident that the response was correct. Each run consisted of 60 responses with symbols presented in random order, except for the fact that symbols were never repeated. We continued training until participants achieved an accuracy of above 95% for both single-finger and chord runs.

After training, participants produced a sequence of chords or single-finger presses at a continuous pace of one response per 2 s. A tone was presented each second, alternating between high-pitch and low-pitch sounds (gray and black notes in Fig. 1*C*, respectively). Participants were instructed to respond simultaneously with high-pitch tones, and the low-pitch tones made the response times temporally more predictable. At a random preparation time of 240–1,750 ms before each high-pitch tone, a symbol appeared on the screen that instructed the required response.

Five single-finger runs were interleaved with five chord runs. Each run consisted of 60 responses. Symbols could occur with equal probability, but no repetitions were allowed. The assignment between symbols and responses was varied across participants (Fig. 1*B*).

Experiment 2. In Experiment 2, participants again produced a sequence of responses synchronized to a sequence of regularly paced tones. These occurred in triplets, at a pace of one tone per 750 ms. The first tone was low-pitch, and the next two were high-pitch, and participants were instructed to synchronize their responses with the two high-pitch tones. On the screen, symbols were presented in two boxes (Fig. 2*A*). The lower box contained the cue for the immediately upcoming response, while the upper box informed participants about future responses. Participants had to produce the two responses in three different conditions: in the overlap condition (Fig. 2*B*), the preparation for the second response overlapped with the execution of the first response. The

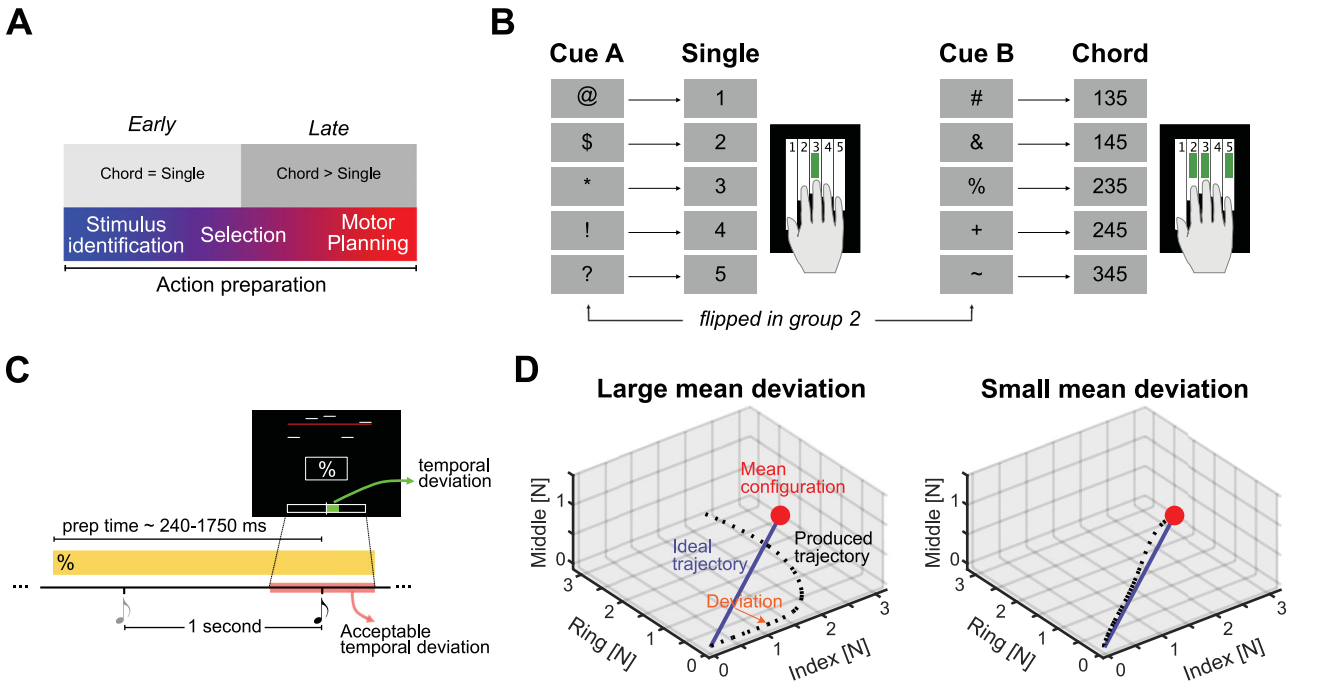

Figure 1. Task design for Experiment 1. ***A***, The cascade of processes constituting action preparation starts with stimulus-related processes (identical for chord and single-finger conditions; early) and ends with movement-related processes (more complex for chords and single-finger movements; late). ***B***, Association between arbitrary cues and actions (single-finger presses and chords). Participants were divided into two groups, and for the second group, the symbol–response assignment was switched across press types. ***C***, Visual stimulus and trial timeline in Experiment 1. Participants needed to produce the action indicated in the box simultaneously with high-pitch tones (black note). The symbol was on the screen during a variable preparation time before the tone (yellow box). Five small lines on the top represented the applied force on each key, with a press threshold of 0.8 N indicated by the red line. ***D***, Example of two produced force trajectories (black dotted lines) with either large (left) or small mean deviations (right) from the ideal force trajectory (purple line). Trials are illustrated in a three-dimensional finger force space consisting of two active fingers (index and ring) and one passive digit (middle).

stimulus for the first symbol appeared 750 ms before the high-pitch tone in the upper box and shifted to the lower box 550 ms before the tone. Simultaneously, the stimulus for the second response appeared in the upper box, allowing the participants a 1,300 ms preparation time for this response. In the nonoverlap conditions, the preparation for the second response did not overlap with the execution of the first response—the stimulus for the second response appeared simultaneously with the tone for the first response. We introduce two variants of the nonoverlap condition: in the nonoverlap short–short (SS, Fig. 2*C*) condition, both responses had a 750 ms preparation time. This condition only differed from the overlap condition by the earlier presentation of the second stimulus. By comparing the behavioral performance for the second response across conditions, we could therefore test whether the participants used the overlap for online planning.

In the nonoverlap long–short (LS, Fig. 2*D*) condition, the first response had a 1,300 ms preparation time. This condition was designed to have the same set of preparation times as the overlap condition, averaged across the two responses. Given that the limited temporal resolution for fMRI forced us to average activity across each pair of responses, this condition provided a strong comparison to the overlap condition. If the activity in these two conditions only differed by the relative timing of the preparation and execution processes, the temporally averaged activity should be identical.

To train the participants in the task, we conducted a behavioral session before the scanning session. At the beginning of this training session, participants were familiarized with the symbol-to-action mapping, as done in Experiment 1. We then trained participants on a simpler version of the task, giving them a 1,300 ms preparation time for both responses (the first response was like nonoverlap LS, and the second response was like overlap). Each pair of responses is repeated eight times (with random symbol pairs each time), resulting in the 16 responses forming a single 18.75 s cycle (2.250 × 8 s plus an extra 750 ms at the beginning). Before each cycle started, a 5 s instruction screen displayed either "Single" or "Chord" to indicate the press type to participants. Each training run comprised three cycles of single-finger presses and three cycles of chords. Participants completed four runs for this phase of training.

Subsequently, participants were trained in the six conditions of the experiment (overlap, nonoverlap SS, nonoverlap LS) × (single-finger, chord). Similarly to training, these were presented in cycles of 16 responses. Before each cycle, a 5 s instruction screen was presented, indicating the upcoming press type (but not the overlap condition). Each run included two cycles of each condition (randomly interleaved), totaling 192 responses. Participants completed six runs during training.

On the day after, participants underwent an fMRI session consisting of 10 runs and one anatomical scan. Similar to training, each run consisted of two cycles of each condition, with each cycle preceded by a 5 s instruction screen. The order of conditions was random. Additionally, two periods of 15 s rest, each preceded by a 5 s "fixate" screen, were placed randomly between conditions. Also, periods of 10 s rest were added at the beginning and the end of each functional run. The rest periods allowed for a better estimation of the baseline activation. Each of the 10 functional runs took ~6 min, and the entire scanning session (including setup and anatomical scan) lasted for ~100 min.

Behavioral data analysis. We evaluated the state of preparation using two different metrics. To assess whether the subjects had selected the correct finger or chord, we calculated the average accuracy. An action was considered accurate if at the peak force time—when the combined force of all five fingers was at its maximum—the force exerted by each active finger was greater than that exerted by each passive finger.

To focus on action-related processes, we determined how well the selected chord was executed. This analysis was restricted to correct trials only. We quantified the execution quality by evaluating the force trajectory in five-dimensional finger space from response initiation to peak force. To determine the initiation time, we calculated the first derivative of the summed force (across all fingers) and then determined the moment that the rate of force change exceeded 5% of the maximum rate within that trial. If the active fingers were pressed simultaneously and the passive fingers

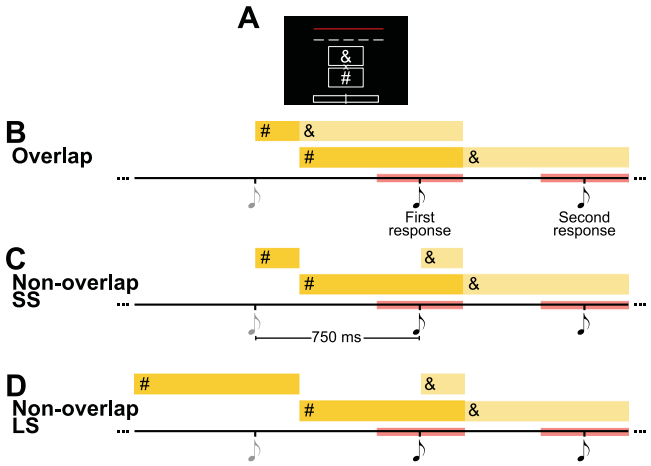

Figure 2. Task design for Experiment 2. ***A***, Visual display. Participants were instructed to produce the action indicated by the symbol in the bottom box. The content of the top box indicated the next action. Participants were instructed to fixate the cross between the two boxes, such that each symbol (~1° from fixation) could be identified without shifting gaze. ***B***, Time course of the continuous paradigm. One low-pitch tone (gray note) alternated with two high-pitch tones (black note). Participants had to produce actions indicated in the bottom box synchronously with high-pitch tones with ±200 ms (red intervals). The symbol displayed in the top and bottom box over time is indicated by the top and bottom yellow strip, respectively. In the overlap condition, the second symbol (&) was visible in the top box during the preparation phase of the first response. ***C***, In the nonoverlap SS condition, the second response cue appeared together with the first tone, preventing online preparation. ***D***, In the nonoverlap LS condition, the first response had a long preparation time.

remained stationary, the produced force trajectory would be aligned with the ideal straight-line trajectory (Waters-Metenier et al., 2014). For each action, the ideal force trajectory begins at the finger forces at initiation time and ends at the "mean configuration," which represents the average force profile of that action at the subject's peak force time within correct trials. Sequential presses of active fingers, involuntary coactivation of passive fingers, pressing the wrong fingers, and initial errors that were later corrected all cause deviation from the ideal straight-line trajectory (Fig. 1*D*). We therefore quantified the accuracy as the Euclidian norm between the produced force and the projection of the produced force onto the straight-line trajectory. This distance was averaged over all time points from the initiation until the peak time to produce the "mean deviation."

To provide an estimation of the necessary preparation time in Experiment 1, we calculated the accuracy as a function of the preparation time separately for each participant and for single-finger and chord. We then fitted the data separately for each subject and each press type with the following function:

$$\hat{y}_n = \frac{d-c}{1+\exp\left(-ax_n+b\right)}+c,$$

where y_n is the predicted accuracy when the preparation time is x_n and a, b, c, and d are free parameters determining, respectively, the slope, the shift, minimum accuracy, and maximum accuracy of the function. Parameters were then fitted to the data of the press type separately using MATLAB's fminsearch routine to minimize the mean squared error loss function. The required preparation time was estimated as the x value for which the predicted accuracy reached 80%.

Statistical analyses on the required preparation time, accuracy, and mean deviation were performed using two-tailed paired–sample t tests and a within-subject repeated–measure ANOVA with factor conditions and press types.

Imaging data acquisition. High-field fMRI data were acquired on a 7 T Siemens Magnetom MRI scanner with a 32-channel head coil at Western University. The anatomical T1-weighted scan of each participant was acquired halfway through the scanning session (after the first five functional runs) using a magnetization-prepared rapid gradient echo sequence with an isotropic voxel size of 0.75 mm [field of view, 208 × 157 × 110 mm (A–P, R–L, F–H), encoding direction coronal]. To measure the BOLD responses in human participants, each functional scan (352 volumes) used the following sequence parameters: GRAPPA 3; multiband acceleration factor 2; repetition time (TR), 1.0 s; echo time (TE), 20 ms; flip angle (FA), 30°; 46 slices; and 2.3 mm isotropic voxel size. To estimate and correct for magnetic field inhomogeneities, we also acquired a gradient echo field map (transversal orientation, field of view, 210 × 210 × 160 mm; 64 slices; 2.5 mm thickness; TR, 475 ms; TE, 4.08 ms; FA, 35°).

Preprocessing and first-level analysis. Data analysis was performed using SPM12 (http://www.fil.ion.ucl.ac.uk/spm/) and custom-written MATLAB (MathWorks) routines. Images were corrected for field inhomogeneities and head motion (Hutton et al., 2002). Due to the short TR (1 s), we did not adjust images for the sequence of slice acquisition. The data were high-pass filtered to remove slowly varying trends with a cutoff frequency of 1/128 Hz and coregistered to the individual anatomical scan. No smoothing or normalization to a group template was implemented during preprocessing.

The preprocessed images were analyzed with two different general linear models (GLMs): the first was designed to estimate how much each of the six task conditions (overlap, nonoverlap SS, nonoverlap LS) × (single-finger, chord) activated each voxel in each of the 10 functional runs. In the design matrix, the regressor for each condition consisted of two boxcar functions (1 for each cycle of 16 responses; length, 18.75 s). We also added a single regressor for instruction periods that happened before each cycle or fixation period (2 s length boxcar functions). The estimate of this regressor was not used in further analysis.

We used a second GLM to estimate the pattern corresponding to each of the 10 actions (five single-finger presses and five chords, Fig. 1*A*) within each run by modeling the first and the second response separately for each action but averaged across all responses and conditions. Each regressor therefore modeled ~20 events of a particular action occurring (16 responses per sequence × 2 repetitions of each sequence × 3 conditions per press type/five action types). The length of boxcar functions varied depending on the available preparation time. We used 1.8 s for the second response in the overlap condition and the first response in the nonoverlap LS condition (Fig. 2*B*,*D*, respectively) and 1.25 s for the rest. The instruction regressor was treated the same as in the first GLM.

The boxcar functions were convolved with an individual-specific hemodynamic response function (HRF). For each participant, we tested which of the 20 HRF functions drawn from the GLMsingle library (https://github.com/cvnlab/GLMsingle/) maximized the proportion of the variance that the model could explain of the time series of voxels in the left primary motor and dorsal premotor cortex (PMd). The selected HRF was then applied to the whole brain. For HRF selection, we treated all conditions as one condition; therefore, this procedure did not bias any subsequent analysis that concerned differences between conditions. Ultimately, the first-level analysis resulted in one activation image (β values) per condition per run. We then calculated the percent signal change for each condition relative to the baseline activation for each voxel for each functional run and averaged it across runs.

Surface-based analysis. Individual subject's cortical surfaces were reconstructed using FreeSurfer (Dale et al., 1999). Individual white–gray matter and pial surfaces were extracted and spherically morphed to match a group template atlas based on the sulcal depth and local surface curvature information (Fischl et al., 1999). Subsequently, surfaces were resampled to a left–right symmetric template (fs_LR32k; Van Essen et al., 2012) included in the connectome workbench distribution (Marcus et al., 2011) using the surfAnalysis toolbox (surf_resliceFS2WB.m, https://github.com/DiedrichsenLab/surfAnalysis). Individual data were then projected onto the group map via the individual surface using the surf_vol2surf.m function in the surfAnalysis toolbox.

Regions of interest (ROIs). We identified 10 ROIs (Fig. 5*A*) based on the cortical areas defined in Glasser et al. (2016) to cover the main anatomical areas that exhibited task-related activations in general (Fig. 5*B*).

These ROIs included the supplementary motor area (SMA), the PMd, the ventral premotor cortex (PMv), the primary motor cortex (M1), the primary somatosensory cortex (S1), the anterior and posterior superior parietal lobules (SPLa/SPLp), the MT+ complex and neighboring visual areas (MT+), the ventral stream visual cortex (VSVC), and the early auditory cortex (EAC).

The SMA was defined as the medial aspect of Brodmann area (BA) 6, covering supplementary and cingulate eye field, 6ma, and 6mp. The PMd was located at the junction between the superior frontal and precentral sulci in the lateral aspect of BA 6, covering 6a, 6d, and frontal eye field. The PMv covered 6v, PEF, and 55b. The M1 ROI covered BA 4; cut 2 cm above and below the hand knob area (Yousry et al., 1997) to restrict it to the cortical hand area. The S1 was defined similarly as the hand-related aspect of BA 1, 2, and 3. The superior parietal cortex was divided into an anterior region (SPLa) covering AIP, 7PC, LIPv, and LIPd and a posterior region (SPLp) covering MIP, VIP, and 7PL. The MT+ covered areas in the lateral occipital and posterior temporal cortex, including LO1, LO2, LO3, V3CD, V4t, FST, MT, MST, and PH. The VSVC lies around the ventral aspect of the left hemisphere, covering areas anterior to early visual areas such as FFC, VVC, V8, VMV1, VMV2, VMV3, and PIT. The EAC includes A1, LBelt, MBelt, PBelt, and RI. The ROIs were defined on the group surface and then projected into the individual space via the cortical surface reconstruction of that individual using the Region toolbox (https://github.com/DiedrichsenLab/region). We selected all voxels that lay between the individual pial and white matter surfaces as part of the ROI.

Additionally to the ROI analysis, we also performed a continuous searchlight analysis (Oosterhof et al., 2011). A searchlight was defined for each surface node, encompassing a circular neighborhood region containing 100 voxels. The voxels for each searchlight were found in exactly the same way as for the ROI definition. As a slightly coarser alternative to searchlights, we also defined a regular tessellation of the cortical surface separated into small hexagons (cortical patches) and extracted the functional data in the same way.

Analysis of activation. We calculated the percent signal change for each condition relative to the baseline value for each voxel for each functional run and averaged it across runs. For the ROI analysis, the percent signal change was averaged across all voxels in the predefined regions in the native volume space of each subject. Additionally, for visualization, the volume maps were projected to the surface for each subject and averaged across the group in the Workbench space.

Statistical analyses to assess differences in percent signal change were conducted using two-tailed paired–sample t tests and within-subject repeated–measure ANOVA with factors conditions (overlap, nonoverlap LS) and press types. Statistical tests on the surface were conducted using an uncorrected threshold of $p = 0.001$, and the familywise error was controlled by calculating the size of the largest superthreshold cluster across the entire cortical surface with estimated smoothness of FWHM 11.4 mm that would be expected by chance ($p = 0.05$) using Gaussian field theory as implemented in the fmristat package (Worsley et al., 1996).

Dissimilarities between activity patterns for responses. To evaluate which regions displayed cue- or action-specific representation, we calculated cross-validated Mahalanobis dissimilarities between the patterns of estimated activities (β values). We first prewhitened the β values: we estimated the voxel noise covariance matrix from the residuals of the GLM and used optimal shrinkage toward a diagonal noise matrix (Ledoit and Wolf, 2003). We then divided the patterns by the matrix square root of this estimate. Multivariate prewhitening has been found to increase the reliability of dissimilarity estimates (Walther et al., 2016). Next, we calculated the cross-validated Mahalanobis dissimilarities (i.e., the crossnobis dissimilarities; Diedrichsen et al., 2020) between evoked regional patterns of different pairs of actions, separately for five single-finger presses and five chords, resulting in a total of 2×10 dissimilarities. To obtain a measure of overall encoding, we averaged these 20 dissimilarities within each cortical surface searchlight area (Oosterhof et al., 2011).

Model-based representational fMRI analysis. While the searchlight analysis tells us from which brain areas we can decode response identity, it does not reveal which specific aspects of the action are represented. We therefore tessellated the area with significantly positive dissimilarities using a discrete set of surface patches and then estimated the contribution of two different representational models within each patch using the pattern component modeling (PCM; Diedrichsen et al., 2011). The two representational components corresponded to a cue and motor representation, respectively. Because we do not a priori know what similarities to predict for the two components, we used the data from a group of subjects with the opposite cue-to-action assignment. We predicted that if a region represented the visual cue, the similarity between patterns should be the same as observed in the other group for the same cues (but different actions). Conversely, if a region represented the action, the pattern similarity should be the same as observed in the other group for the same action (but a different cue). Thus, we specified the two model components for Group 1 from the average data from Group 2 in the same area (and vice versa).

Based on these two components, we then formulated a model family containing all possible combinations of the two representational components (Yokoi and Diedrichsen, 2019). This resulted in four combinations, also containing the "null" model that predicated no differences among any of the activity patterns. We evaluated all four models using a cross-validated leave-one-subject-out scheme because different combination models had different numbers of free parameters. The component weights were fitted to maximize the likelihood of the data of $N-1$ subjects. We then evaluated the likelihood of the observed activity patterns for each cortical patch [in volume space, see above, Regions of interest (ROIs)] of the left-out subject N under that model. The resultant cross-validated likelihoods were used as an estimate of model evidence for each of the four models (Diedrichsen et al., 2018). The log Bayes factor BF_m, the difference between the cross-validated log-likelihood of each model and the null model, characterizes the relative evidence for that model.

The log Bayes factor for each model component was calculated as the log of the ratio between averaged likelihood for the models that contained the component ($c = 1$) versus the averaged likelihood for the models that did not ($c = 0$ Shen and Ma, 2019):

$$\mathrm{logBF_c} = \log\left(\frac{\frac{1}{N_{m:c=1}}\sum_{m:c=1}\exp(\mathrm{logBF}_m)}{\frac{1}{N_{m:c=0}}\sum_{m:c=0}\exp(\mathrm{logBF}_m)}\right),$$

where $N_{m:c=1}$ ($N_{m:c=0}$) denotes the number of models (not) containing the component. Thus, a positive log Bayes factor indicated that there was evidence for the presence of the component. The analysis was performed separately for the two groups of subjects and for single and chord data. As chord and single datasets were independent, we finally summed the log Bayes factors for the corresponding components within each individual. Lastly, we projected the log Bayes factors of each cortical patch onto the vertices associated with that patch to create a cue and an action encoding map.

Statistical analysis of PCM. Within each cortical patch, the final log Bayes factors for cue and action components for each participant were then submitted to a Bayesian group analysis, which estimates the probability that the component is present in a given subject (Stephan et al., 2009; Rosa et al., 2010; spm_BMS function implemented in the SPM 12). The significance was assessed using the protected exceedance probability (PXP)—the posterior probability that a component is present in more than half of the participants. We deemed a model contribution significant when PXP is larger than 0.75.

Results

Complex actions require longer preparation time

In Experiment 1, we measured the time necessary to prepare a single-finger or chord press. The first part of action preparation (Fig. 1*A*, stimulus identification, selection of an action)

should be matched across the two conditions, as we counterbalanced the assignment of symbols to actions (Fig. 1*B*). Thus, any differences in the required preparation time could be attributed to the second part of action preparation (selection of fingers involved in a chord, planning the corresponding motor action).

When there was not enough time to prepare an action, accuracy was at chance level (20%) for both single fingers and chords. When the available preparation time increased, accuracy reached almost perfect performance: 95 ± 1% for single fingers and 90 ± 1% for chords (Fig. 3*A*, a significant difference, $t_{10} = 5.387$; $p = 2.2 \times 10^{-4}$). After fitting a logistic function to the data (see Materials and Methods, Behavioral data analysis), we found it took longer for chords (849 ± 43 ms) to reach the accuracy of 80% than for single fingers (580 ± 18 ms), a significant difference ($t_{(10)} = 5.918$; $p = 1.5 \times 10^{-4}$). The extra 270 ms preparation time can be attributed to recalling a more complex memory representation for the chords and/or to plan a more complex motor action.

Even when only looking at the correct trials, we found that the quality of the chord execution improved with increasing preparation time (Fig. 3*B*). As a measure of movement quality, we analyzed the mean deviation of each chord (see Materials and Methods, Behavioral data analysis), a measure that captures how synchronous the active finger produced the forces and how still the passive fingers remained. For correct chords, the mean deviation decreased as a function of the preparation time. Specifically, correct chords with a preparation time of shorter than 800 ms showed a significantly higher mean deviation than correct chords with a preparation time exceeding 800 ms; $t_{(10)} = 6.228$; $p = 1.0 \times 10^{-4}$. For single-finger movements, no such difference was found; $t_{(10)} = 0.906$; $p = 0.3864$. This suggests that for chords, participants could improve the quality of execution with the extended preparation time, even after they had selected the correct finger configuration.

Online preparation improves the second action in the overlap condition

In the main experiment (Experiment 2), we aimed to create a condition in which participants would prepare for the next action while still executing the previous one. To do so, we selected a time between two consecutive responses that was not enough to fully prepare a chord and barely enough to prepare a single-finger press. Based on the results from Experiment 1, we chose an interval of 750 ms. We hypothesized that if the stimulus for the second action was presented before the first response was completed, participants would utilize that information to improve their execution quality.

If this hypothesis was correct, the second response should be executed more accurately in the overlap than in the nonoverlap conditions. Before testing this idea, however, we needed to ensure that the second stimulus in the overlap condition did not interfere with the first action. For chords, this was indeed the case: the first response was equally accurate in the overlap and in the nonoverlap SS condition (Fig. 4*A*; $t_{(21)} = 0.191$; $p = 0.8507$). As predicted from Experiment 1, the first response was much more accurate in the nonoverlap LS condition (both for chord and single, $t_{(21)} > 3.551$; $p < 0.0019$). This difference could simply be explained by the longer preparation time for the first response. For single-finger actions, the accuracy was overall higher, and the benefit of a longer preparation time was smaller than for chords, as shown by a significant condition × press type interaction ($F_{(1,21)} = 6.260$; $p = 0.0042$).

Critically, we confirmed that the participants used the earlier appearance of the second cue in the overlap condition for online preparation. For both chords and single-finger presses, the accuracy for the second response was larger in the overlap than that in the nonoverlap SS (chord, $t_{(21)} = 4.282$; $p = 0.0003$; single, $t_{(21)} = 5.072$; $p = 5.0 \times 10^{-5}$) and the nonoverlap LS condition (chord, $t_{(21)} = 2.967$; $p = 0.0073$; single, $t_{(21)} = 2.958$; $p = 0.0075$). Thus, online preparation provided an advantage for both chords and single-finger presses, with a larger benefit for chords ($t_{(21)} = 2.213$; $p = 0.03814$).

The benefit of being able to plan online can also be seen in the execution quality of correct chords only (Fig. 4*B*). The second response had a smaller mean deviation in the overlap than that in the nonoverlap SS condition ($t_{(21)} = 2.530$; $p = 0.0195$). Thus, online preparation improved the selection accuracy and execution quality of the upcoming response, and this benefit was more apparent for complex actions.

Online preparation activates the superior parietal lobule and ventral visual stream but not the premotor areas

To examine which brain regions are more activated in online preparation, we compared the fMRI activation during the overlap versus the nonoverlap conditions. Because it is challenging to separate the fMRI activity related to the first and second response, our estimates of activity were temporally averaged across multiple pairs of responses. If processes related to the preparation and execution of actions occurred independently

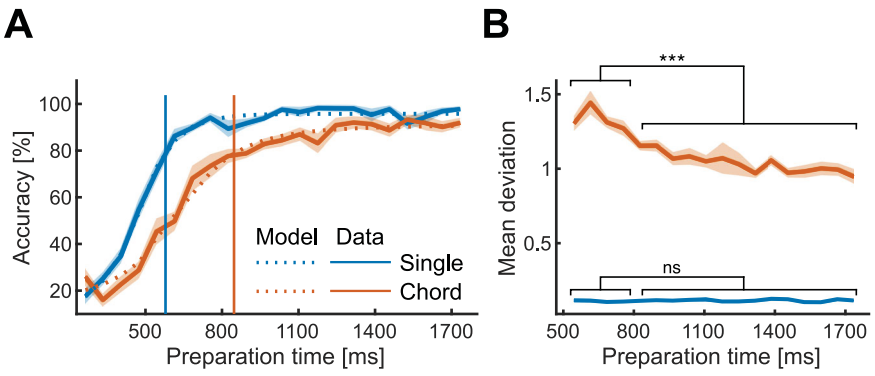

Figure 3. Three-finger chords take longer to prepare. ***A***, Solid lines indicate the group-averaged accuracy as a function of available preparation time for single (blue) and chord (orange). The dotted lines are the model fit average across subjects. The vertical lines indicate the median time when the fitted curves for chord (orange) or single finger (blue) reach 80%. ***B***, Similar to ***A*** but for mean deviation. Significant pairwise differences are indicated with ***$p < 0.001$, ns (not significant), $p > 0.05$, in a two-sided one–sample t test.

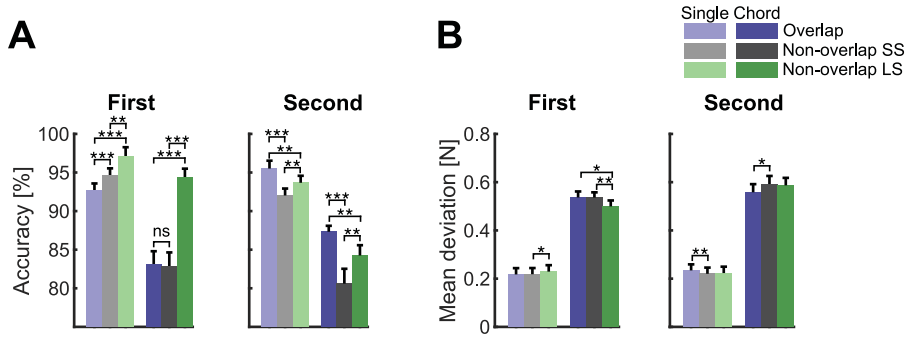

Figure 4. Online preparation benefits execution. ***A***, Accuracy for the first (left) and the second response (right) separate for single-finger and chord and overlap and nonoverlap conditions. ***B***, Mean deviation from a straight-line force trajectory within correct trials for the first response (left) and second response (right) separate for single-finger and chord and overlap and nonoverlap conditions. Error bars indicate the SEM across participants. ***$p < 0.001$, **$p < 0.01$, *$p < 0.05$, using two-sided paired t test.

in different neuronal populations, then the overlap (Fig. 2*B*) and the nonoverlap LS condition (Fig. 2*D*) would be exactly matched for the type of processes that occur (two executions, one long preparation, one short preparation)—they only differ in the relative timing of their occurrence. Consequently, the temporally averaged activity in these two conditions should be identical. Hence, any difference in BOLD activation between the two conditions can be attributed to differences between the online preparation in the overlap condition and the preparation of an isolated response in the nonoverlap condition.

Averaged across single fingers and chords and compared with rest, the task activated the primary and secondary sensorimotor cortices, regions along the intraparietal sulcus, areas in the occipitotemporal cortex, and the auditory cortex (Fig. 5*A*,*B*). Within this task-relevant network, we found that only areas in the superior posterior lobule (SPLa, $F_{(1,21)} = 10.879$; $p = 0.0034$; SPLp, $F_{(1,21)} = 10.684$; $p = 0.0037$) and in the ventral visual stream (MT+, $F_{(1,21)} = 64.708$; $p = 7.5 \times 10^{-8}$; VSVC, $F_{(1,21)} = 39.777$; $p = 3.0 \times 10^{-6}$) were more activated during online preparation (Fig. 5*C*,*E*). This was also clear in the surface-based analysis, in which the largest significant clusters ($p = 8.0 \times 10^{-7}$; corrected for multiple comparisons; see Materials and Methods, Surface-based analysis) extended from the intraparietal sulcus to visual areas on the boundary between occipital and temporal lobe (dashed back line, Fig. 5*C*).

Interestingly, we did not find any evidence of extra activation during online preparation in premotor areas. Neither the PMd ($F_{(1,21)} = 0.807$; $p = 0.3791$) nor the SMA ($F_{(1,21)} = 0.314$; $p = 0.5812$) was significantly more active during the overlap condition. This null-finding was not due to lacking power in these areas—the ROI × condition effect involving either all 10 regions (Fig. 5*A*; $F_{(9,189)} = 22.498$; $p < 1.0 \times 10^{-10}$) or only PMd versus SPLa ($F_{(1,21)} = 25.708$; $p = 5.0 \times 10^{-5}$) was highly significant. These results demonstrate an important dissociation, with posterior parietal, but not frontal premotor, areas showing more activation during online preparation.

Action complexity increases activity in both premotor and parietal areas

The observed dissociation is all the more surprising given the well-established role of both the posterior parietal and frontal premotor areas in motor planning of hand and arm movements (Tanji and Shima, 1994; Hoshi and Tanji, 2004; Gallivan et al., 2011, 2016; Shenoy et al., 2013; Henderson et al., 2022). Consistent with this idea, we found much higher activity for the chord as compared with the single-finger condition (Fig. 5*D*) both in premotor (Fig. 5*E*, PMd, $F_{(1,21)} = 77.716$; $p = 1.6 \times 10^{-8}$; PMv, $F_{(1,21)} = 33.580$; $p = 9.4 \times 10^{-6}$; SMA, $F_{(1,21)} = 48.361$; $p = 7.2 \times 10^{-7}$) and superior parietal areas (SPLa, $F_{(1,21)} = 105.196$; $p = 1.2 \times 10^{-9}$; SPLp, $F_{1,21} = 62.366$; $p = 1.0 \times 10^{-7}$).

This difference was not present in areas related to the processing of auditory signals (EAC, $F_{(1,21)} = 2.331$; $p = 0.1418$). Somewhat surprisingly, however, we found that activity in the lateral occipitotemporal cortex was modulated by the complexity of the motor response (MT+, $F_{(1,21)} = 30.202$; $p = 1.8 \times 10^{-5}$; VSVC, $F_{(1,21)} = 27.710$; $p = 3.2 \times 10^{-5}$). This was despite the fact that chord and single-finger conditions were matched in terms of the visual information.

Online preparation activity does not vary with action complexity

What processes cause the extra activity during the overlap condition in the posterior parietal cortex? If these processes were related to motor planning, we predicted that overlapping preparation would be harder if motor planning takes longer; consequently, the overlap versus nonoverlap difference should be larger for chords. This was not the case, however. The activity overlap versus nonoverlap difference for single-finger movements (Fig. 6*A*) and chords (Fig. 6*B*) was roughly equivalent. Indeed, we find a significant condition × press type interaction in none of the regions that showed higher activity in the overlap versus nonoverlap condition (Fig. 5*E*; $F_{(1,21)} < 1.004$; $p > 0.3884$). This suggests that the extra activity in these areas was not related to later phases of action preparation (i.e., motor planning) but rather to the earlier phases, associated with cue identification and action selection, independent of the exact details of the motor program (Fig. 1*A*).

Action versus cue encoding across task-related areas

Finally, we sought to characterize where on the continuum from cue to action-related processes each task-related area falls (Fig. 1*A*). To achieve this, we characterized the features that are represented in the fine-grained patterns of activity in these regions that used multivoxel pattern analysis: we estimated the activity patterns for the 10 possible actions (five different singles and five chords) by modeling the first and second responses separately and averaging across all responses and conditions (see Materials and Methods, Preprocessing and first-level analysis). We determined the dissimilarity of the patterns associated with the five responses, resulting in a representational dissimilarity matrix (RDM) for each press type (single finger vs chords) and each area separately (Fig. 7*A*,*B*). We then asked to what degree the similarity between activity patterns can be explained by the

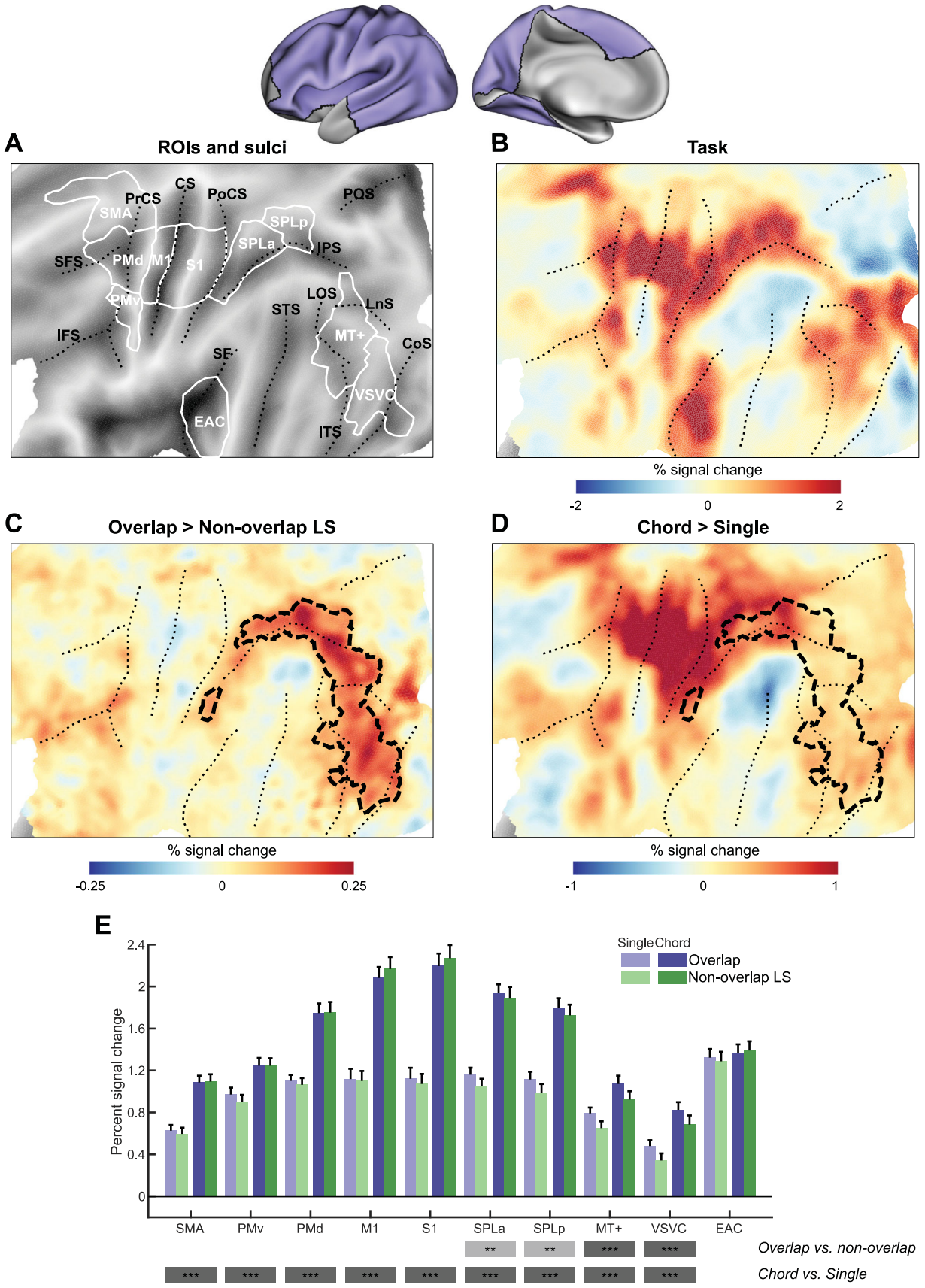

Figure 5. Online preparation activates superior parietal and occipitotemporal regions. The inset shows the inflated cortical surface of the contralateral (left) hemisphere, highlighting the area of interest (***A***–***C***, purple). ***A***, Flat representation of the neocortex with major sulci indicated by black dotted lines and ROIs by white borders. ***B***, Group-averaged percent signal change for task versus resting baseline averaged across overlap and nonoverlap conditions and press types (single, chord). ***C***, The difference in percent signal change between overlap and nonoverlap LS conditions, averaged across single finger and chord. Black dashed boundaries represent significant clusters. ***D***, The activity difference between chord and single-finger conditions. The dashed

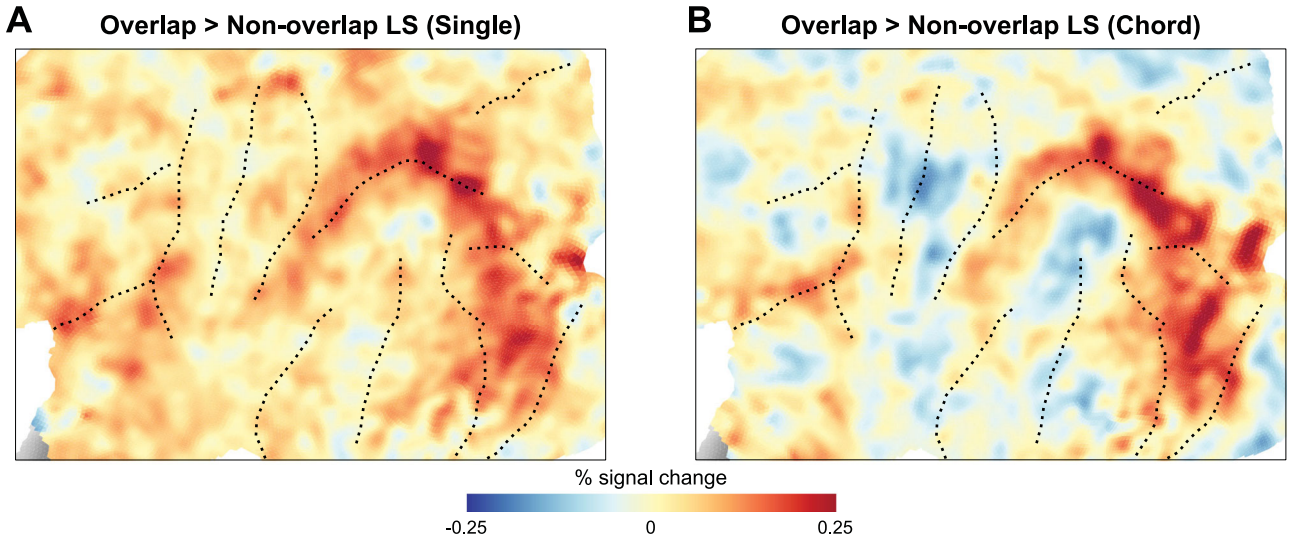

Figure 6. No evidence for extra online preparation activation in chord conditions. ***A***, The contrast between the overlap and nonoverlap condition for single fingers and (***B***) for chords.

similarity between visual cues or the similarity between actions. As a model, we used the data from the other half of the participants, for which the assignment between visual cues and actions was switched (Fig. 1*B*). For example, as a model for the similarity of patterns within SPLa, we used the average similarities between the same actions within SPLa of the other half of the participants as a model for action-related processes. Additionally, we used the average similarities between the same cues (for different actions) within SPLa as a model for cue-related processes. To be able to model combinations of both cue- and action-related processes, we used a Bayesian model family approach (Yokoi and Diedrichsen, 2019), which evaluates the evidence for each model component (cue or action) in the context of the other component.

As expected, in the M1, the RDM for one-half of the participants was similar to the RDM for the other half of the participants when matching the action but not the cue (Fig. 7*A*). Such action-related encoding was shown in M1, S1, and PMd, with the subject-averaged log Bayes factor for action providing strong evidence for action encoding (Fig. 7*C*). This is consistent with the role of PMd in motor planning and execution (Shenoy et al., 2013).

In contrast, the RDM for the same actions in MT+ matched the RDM from the other half of the subjects when using the same cue, but not action (Fig. 7*B*). Evidence for cue encoding was found in all visual areas including VSVC and MT+ (Fig. 7*D*). The finding that VSVC and MT+ represented the cue is consistent with the literature indicating that these areas represent shapes (Glasser et al., 2016; Wurm and Caramazza, 2022).

The areas along the intraparietal sulcus also showed evidence of action-related encoding. Together with the visual areas, these areas were part of the cluster that was more highly activated during online preparation (dashed outline in Fig. 6*C*,*D*). Within this cluster, we found 14 cortical patches with significant action encoding and 10 cortical patches with significant cue encoding.

Discussion

The brain regularly needs to generate rapid sequences of actions, often requiring the preparation of future actions while still executing the ongoing action. In this paper, we asked how this problem is solved at the whole-brain level. We found an unexpected dissociation: superior parietal and occipitotemporal regions were more activated when actions overlapped, whereas premotor areas did not show any extra activity. This dissociation is remarkable in that both superior parietal lobule (SPL) and PMd are thought to be involved in motor planning. fMRI studies have reported that activity patterns in these two areas encode very similar information, including the intended effector (Gallivan et al., 2013; Leoné et al., 2014) and the planned sequences of future actions (Gallivan et al., 2016; Yokoi and Diedrichsen, 2019; Berlot et al., 2021). Electrophysiological recordings have also consistently shown that patterns of neural activity in both areas encode details of the upcoming movement (Wise et al., 1986; Kalaska, 1988; Kalaska et al., 1990; Kalaska and Crammond, 1995; Scott et al., 1997; Cisek and Kalaska, 2005; Nakayama et al., 2008; Kaufman et al., 2010). In our study, we found higher activity during the motorically more complex chords than during single-finger presses in both areas. Furthermore, multivariate analyses showed clear evidence for action encoding, confirming the involvement of both regions in motor planning in our task. Nonetheless, we found increased activity during the action overlap in SPL but not in PMd.

This finding may have two explanations. First, online planning may have occurred in PMd in our task but in such a way that it

←

outline is the same as in ***C***. ***E***, ROI-based analysis of percent signal change across overlap (purple)/nonoverlap (green) LS conditions for chords (dark) and single-finger presses (light). Error bars denote SEM across participants. Bars at the bottom of this panel show the significance of overlap versus nonoverlap LS effect and chord versus single effect within each region (dark gray, ***$p < 0.001$; light gray, **$p < 0.005$). ROIs: early auditory cortex (EAC), ventral stream visual cortex (VSVC), MT+ complex and neighboring visual areas (MT+), posterior superior parietal lobule (SPLp), anterior superior parietal lobule (SPLa), primary somatosensory cortex (S1), primary motor cortex (M1), dorsal premotor cortex (PMd), ventral premotor cortex (PMv), secondary motor area (SMA). Sulci: superior frontal sulcus (SFS), inferior frontal sulcus (IFS), precentral sulcus (PrCS), central sulcus (CS), postcentral sulcus (PoCS), intraparietal sulcus (IPS), parieto-occipital sulcus (POS), lateral occipital sulcus (LOS), lunate sulcus (LnS), superior temporal sulcus (STS), inferior temporal sulcus (ITS), collateral sulcus (CoS), sylvian fissure (SF).

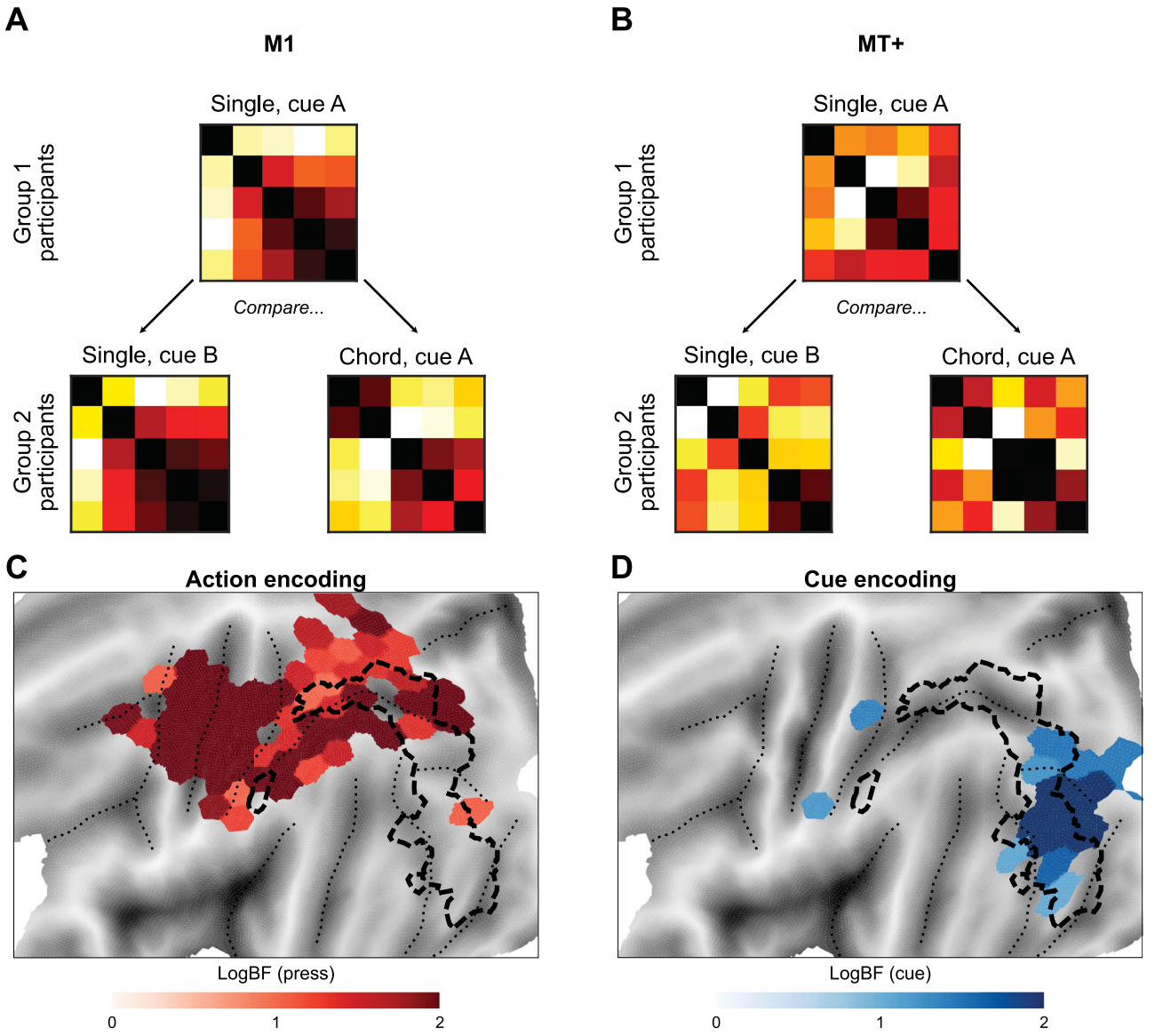

Figure 7. Involvement of task-related network in cue-related and action-related processes. ***A***, The average RDM for of group 1 was compared with the average RDM of Group 2 for actions with the same press type (left) or with the same set of cues (right). For M1, the similarity was high when the actions were matched. ***B***, In MT+ region, the similarity was higher when the cues were matched. ***C***,***D***, Group maps for the log Bayes factor for the action model (***C***) and cue model (***D***). Darker colors represent stronger evidence for encoding. Each map was thresholded with PXP >0.75 and log Bayes factor (logBF) >1. Black dashed outline is the same as in Figure 5*C*.

could run in parallel with ongoing execution without requiring extra activity. It has been suggested that neural patterns in M1 and PMd underlying movement preparation occur in orthogonal neural dimensions to the ones supporting the motor execution (Kaufman et al., 2014; Elsayed et al., 2016). Under this arrangement, activity along the movement preparation dimensions does not interfere with the ongoing execution (Zimnik and Churchland, 2021). Indeed, if neural activity for preparation and execution would superimpose additively, we would predict that the temporally averaged activity in the overlap and the non-overlap LS conditions (which only differ in the relative timing of these processes) would be equivalent.

Alternatively, however, PMd may not have been involved in online preparation in our task at all. Recent electrophysiological results, however, have demonstrated that both ongoing and upcoming movements are represented at the same time in PMd (Zimnik and Churchland, 2021). These results were found in a task that involved reaching spatial targets, whereas our task used an arbitrary stimulus-to-response mapping, which may have increased the importance of cue identification and action selection processes. It is an open question whether the direct mapping between cues and actions (Diedrichsen et al., 2001) would heighten online planning processes in PMd and may even cause increased activity during overlapping actions. However, given the clear involvement of PMd in planning actions based on arbitrary cues (di Pellegrino and Wise, 1993), we think it is more likely that online preparation did indeed occur in PMd in our task, as it does during goal-directed reaching.

In contrast to PMd, we found clear evidence of increased activity during online preparation in SPL. There is evidence that SPL is involved in motor planning (Gallivan et al., 2013; Leoné et al., 2014) but also that it represents the goal of upcoming actions independently of the exact motor requirements (Hamilton and Grafton, 2006; Henderson et al., 2022;

Shushruth et al., 2022). Increased activity during the overlap condition could therefore be attributed to interference at either stage. However, the fact that the increase was not larger in the chord than that in the single-finger condition seems to be at odds with interference arising at the stage of motor planning. We would have expected that when motor planning requires more time, any interference would require more activity to be resolved. Therefore, the extra activity is more likely attributed to processes preceding detailed motor planning. Neurophysiological studies have shown that SPL represents different potential actions in the form of a priority map (Bisley and Goldberg, 2010). Thus, it is possible that the selection of the two simultaneously ongoing actions causes interference, and an increase in activity is required to resolve this conflict.

Widespread increases in activity were also found in the occipitotemporal cortex. Multivariate analysis confirmed that these regions represent the visual cue but not the identity of the action. When actions overlap, the brain needs to identify the visual cue of the ongoing and next actions simultaneously. This dual task likely requires the allocation of additional attentional resources (Pashler, 1999), which would explain the increased neuronal activity. Interestingly, the activity in these visual regions was also slightly higher in the motorically more complex chords than that in simple finger movements. This is surprising, as the visual and attentional requirements were tightly matched across chord and single-finger conditions. These results suggest that the identification of the visual cue and the process of motor planning do not occur in a strictly serial manner (Cisek and Kalaska, 2010): visual areas may need to maintain the cue representation until motor planning is concluded. This would explain why complex actions that require more motor planning would be associated with higher activity in visual areas.

Taken together, our results suggest that the main bottleneck for online preparation occurs at the stage of cue identification and action selection. Cortical areas in the ventral visual stream need to maintain a representation of the current cue while already identifying the next cue. Similarly, SPL needs to maintain the identity of the ongoing action while selecting the next action goal. These processes likely require more attentional resources when dealing with overlapping tasks (Welford, 1952; Smith, 1968; McLeod, 1977), thereby causing more neuronal activity. Conversely, the lack of extra activity in cortical premotor areas suggests that motor planning can proceed in parallel with ongoing execution, an idea that is consistent with the model of orthogonal subspaces for planning and execution (Kaufman et al., 2014; Zimnik and Churchland, 2021).

References

Ames KC, Ryu SI, Shenoy KV (2014) Neural dynamics of reaching following incorrect or absent motor preparation. Neuron 81:438–451.

Ariani G, Kordjazi N, Pruszynski JA, Diedrichsen J (2021) The planning horizon for movement sequences. eNeuro 8:ENEURO.0085-21.2021.

Berlot E, Popp NJ, Grafton ST, Diedrichsen J (2021) Combining repetition suppression and pattern analysis provides new insights into the role of M1 and parietal areas in skilled sequential actions. J Neurosci 41:7649–7661.

Bisley JW, Goldberg ME (2010) Attention, intention, and priority in the parietal lobe. Annu Rev Neurosci 33:1–21.

Churchland MM, Shenoy KV (2007) Temporal complexity and heterogeneity of single-neuron activity in premotor and motor cortex. J Neurophysiol 97:4235–4257.

Cisek P, Kalaska JF (2005) Neural correlates of reaching decisions in dorsal premotor cortex: specification of multiple direction choices and final selection of action. Neuron 45:801–814.

Cisek P, Kalaska JF (2010) Neural mechanisms for interacting with a world full of action choices. Annu Rev Neurosci 33:269–298.

Crammond DJ, Kalaska JF (1994) Modulation of preparatory neuronal activity in dorsal premotor cortex due to stimulus-response compatibility. J Neurophysiol 71:1281–1284.

Crammond DJ, Kalaska JF (2000) Prior information in motor and premotor cortex: activity during the delay period and effect on pre-movement activity. J Neurophysiol 84:986–1005.

Dale AM, Fischl B, Sereno MI (1999) Cortical surface-based analysis. I. Segmentation and surface reconstruction. Neuroimage 9:179–194.

Diedrichsen J, Berlot E, Mur M, Schütt HH, Shahbazi M, Kriegeskorte N (2020) Comparing representational geometries using whitened unbiased-distance-matrix similarity. Neurons Behav Data Anal Theory 5:1–31.

Diedrichsen J, Hazeltine E, Kennerley S, Ivry RB (2001) Moving to directly cued locations abolishes spatial interference during bimanual actions. Psychol Sci 12:493–498.

Diedrichsen J, Ridgway GR, Friston KJ, Wiestler T (2011) Comparing the similarity and spatial structure of neural representations: a pattern-component model. Neuroimage 55:1665–1678.

Diedrichsen J, Yokoi A, Arbuckle SA (2018) Pattern component modeling: a flexible approach for understanding the representational structure of brain activity patterns. Neuroimage 180:119–133.

di Pellegrino G, Wise SP (1993) Visuospatial versus visuomotor activity in the premotor and prefrontal cortex of a primate. J Neurosci 13:1227–1243.

Elsayed GF, Lara AH, Kaufman MT, Churchland MM, Cunningham JP (2016) Reorganization between preparatory and movement population responses in motor cortex. Nat Commun 7:13239.

Fischl B, Sereno MI, Tootell RB, Dale AM (1999) High-resolution intersubject averaging and a coordinate system for the cortical surface. Hum Brain Mapp 8:272–284.

Gallivan JP, Johnsrude IS, Flanagan JR (2016) Planning ahead: object-directed sequential actions decoded from human frontoparietal and occipitotemporal networks. Cereb Cortex 26:708–730.

Gallivan JP, McLean DA, Flanagan JR, Culham JC (2013) Where one hand meets the other: limb-specific and action-dependent movement plans decoded from preparatory signals in single human frontoparietal brain areas. J Neurosci 33:1991–2008.

Gallivan JP, McLean DA, Valyear KF, Pettypiece CE, Culham JC (2011) Decoding action intentions from preparatory brain activity in human parieto-frontal networks. J Neurosci 31:9599–9610.

Glasser MF, et al. (2016) A multi-modal parcellation of human cerebral cortex. Nature 536:171–178.

Haith AM, Pakpoor J, Krakauer JW (2016) Independence of movement preparation and movement initiation. J Neurosci 36:3007–3015.

Hamilton AFC, Grafton ST (2006) Goal representation in human anterior intraparietal sulcus. J Neurosci 26:1133–1137.

Henderson MM, Rademaker RL, Serences JT (2022) Flexible utilization of spatial- and motor-based codes for the storage of visuo-spatial information. Elife 11:e75688.

Hoshi E, Tanji J (2004) Differential roles of neuronal activity in the supplementary and presupplementary motor areas: from information retrieval to motor planning and execution. J Neurophysiol 92:3482–3499.

Hutton C, Bork A, Josephs O, Deichmann R, Ashburner J, Turner R (2002) Image distortion correction in fMRI: A quantitative evaluation. NeuroImage 16:217–240.

Kalaska JF (1988) The representation of arm movements in postcentral and parietal cortex. Can J Physiol Pharmacol 66:455–463.

Kalaska JF, Cohen DA, Prud'homme M, Hyde ML (1990) Parietal area 5 neuronal activity encodes movement kinematics, not movement dynamics. Exp Brain Res 80:351–364.

Kalaska JF, Crammond DJ (1995) Deciding not to GO: neuronal correlates of response selection in a GO/NOGO task in primate premotor and parietal cortex. Cereb Cortex 5:410–428.

Kashefi M, Reschechtko S, Ariani G, Shahbazi M, Die-drichsen J, Pruszynski JA (2023) Interaction of multiple future movement plans in sequential reaching. bioRxiv:2023.05.24.542099. Available at: https://www.biorxiv.org/content/10.1101/2023.05.24.542099 [Accessed June 3, 2023].

Kaufman MT, Churchland MM, Ryu SI, Shenoy KV (2014) Cortical activity in the null space: permitting preparation without movement. Nat Neurosci 17:440–448.

Kaufman MT, Churchland MM, Santhanam G, Yu BM, Afshar A, Ryu SI, Shenoy KV (2010) Roles of monkey premotor neuron classes in movement preparation and execution. J Neurophysiol 104:799–810.

Ledoit O, Wolf MN (2003) Honey, I shrunk the sample covariance matrix. SSRN Electron J. Available at: https://jpm.pm-research.com/content/30/4/110.short.

Leoné FT, Heed T, Toni I, Medendorp WP (2014) Understanding effector selectivity in human posterior parietal cortex by combining information patterns and activation measures. J Neurosci 34:7102–7112.

Marcus DS, Harwell J, Olsen T, Hodge M, Glasser MF, Prior F, Jenkinson M, Laumann T, Curtiss SW, Van Essen DC (2011) Informatics and data mining tools and strategies for the human connectome project. Front Neuroinform 5:4.

McLeod P (1977) A dual task response modality effect: support for multiprocessor models of attention. Q J Exp Psychol 29:651–667.

Nakayama Y, Yamagata T, Tanji J, Hoshi E (2008) Transformation of a virtual action plan into a motor plan in the premotor cortex. J Neurosci 28:10287–10297.

Oosterhof NN, Wiestler T, Downing PE, Diedrichsen J (2011) A comparison of volume-based and surface-based multi-voxel pattern analysis. Neuroimage 56:593–600.

Pashler H (1999) *The psychology of attention*. MIT Press.

Pruszynski JA, Omrani M, Scott SH (2014) Goal-dependent modulation of fast feedback responses in primary motor cortex. J Neurosci 34:4608–4617.

Rosa MJ, Bestmann S, Harrison L, Penny W (2010) Bayesian model selection maps for group studies. Neuroimage 49:217–224.

Rosenbaum DA, Kornblum S (1982) A priming method for investigating the selection of motor responses. Acta Psychol 51:223–243.

Scott SH, Sergio LE, Kalaska JF (1997) Reaching movements with similar hand paths but different arm orientations. II. Activity of individual cells in dorsal premotor cortex and parietal area 5. J Neurophysiol 78:2413–2426.

Shen S, Ma WJ (2019) Variable precision in visual perception. Psychol Rev 126:89–132.

Shenoy KV, Sahani M, Churchland MM (2013) Cortical control of arm movements: a dynamical systems perspective. Annu Rev Neurosci 36:337–359.

Shushruth S, Zylberberg A, Shadlen MN (2022) Sequential sampling from memory underlies action selection during abstract decision-making. Curr Biol 32:1949–1960.e5.

Smith MC (1968) Repetition effect and short-term memory. J Exp Psychol 77:435–439.

Stephan KE, Penny WD, Daunizeau J, Moran RJ, Friston KJ (2009) Bayesian model selection for group studies. Neuroimage 46:1004–1017.

Tanji J, Evarts EV (1976) Anticipatory activity of motor cortex neurons in relation to direction of an intended movement. J Neurophysiol 39:1062–1068.

Tanji J, Shima K (1994) Role for supplementary motor area cells in planning several movements ahead. Nature 371:413–416.

Van Essen DC, Glasser MF, Dierker DL, Harwell J, Coalson T (2012) Parcellations and hemispheric asymmetries of human cerebral cortex analyzed on surface-based atlases. Cereb Cortex 22:2241–2262.

Walther A, Nili H, Ejaz N, Alink A, Kriegeskorte N, Diedrichsen J (2016) Reliability of dissimilarity measures for multi-voxel pattern analysis. Neuroimage 137:188–200.

Waters-Metenier S, Husain M, Wiestler T, Diedrichsen J (2014) Bihemispheric transcranial direct current stimulation enhances effector-independent representations of motor synergy and sequence learning. J Neurosci 34:1037–1050.

Welford AT (1952) The "psychological refractory period" and the timing of high-speed performance—a review and a theory. Br J Psychol 43:2–19.

Wise SP, Weinrich M, Mauritz KH (1986) Movement-related activity in the premotor cortex of rhesus macaques. Prog Brain Res 64:117–131.

Worsley KJ, Marrett S, Neelin P, Vandal AC, Friston KJ, Evans AC (1996) A unified statistical approach for determining significant signals in images of cerebral activation. Hum Brain Mapp 4:58–73.

Wurm MF, Caramazza A (2022) Two 'what' pathways for action and object recognition. Trends Cogn Sci 26:103–116.

Yokoi A, Diedrichsen J (2019) Neural organization of hierarchical motor sequence representations in the human neocortex. Neuron 103:1178–1190.e7.

Yousry TA, Schmid UD, Alkadhi H, Schmidt D, Peraud A, Buettner A, Winkler P (1997) Localization of the motor hand area to a knob on the precentral gyrus. A new landmark. Brain 120:141–157.

Zimnik AJ, Churchland MM (2021) Independent generation of sequence elements by motor cortex. Nat Neurosci 24:412–424.